ECIO'05: 12th EUROPEAN CONFERENCE ON INTEGRATED OPTICS
- ABSTRACT -

INTEGRATED OPTICAL CHEMICAL SENSING

James S. Wilkinson

Optoelectronics Research Centre
University of Southampton
Highfield, Southampton, Hampshire, SO17 1BJ, UK.
jsw@orc.soton.ac.uk

SUMMARY

Integrated optical techniques offer the potential for miniature, low-cost, reliable microsystems for chemical analysis which may be exploited in monitoring environmental pollution, food contamination, state of health, and threats to security. Some approaches towards providing flexible multisensor platforms for a wide variety of chemical and biochemical species will be presented.

KEYWORDS
integrated optics, chemical sensors, biosensors

INTRODUCTION

Integrated optics has seen unprecedented growth in the past two decades, driven largely by the great success of optical fibre telecommunications. Research into chemical and biological sensors has exploited these advances and produced a significant body of science and technology dedicated to realising integrated optical devices to monitor chemical reactions at surfaces. While the success of optical communications has apparently satisfied demand in long-distance communications for the time being, interrupting the growth in commercialisation of integrated optics in this field, simple optical waveguide devices for bio/chemical sensing are becoming commercially available. As Culshaw has pointed out in a review of optical fibre sensor technologies [1], while in communications many people are doing much the same thing, in sensing there are many very different quantities to measure so that the market is fragmented and the technological solutions vary widely, making the field less attractive for large enterprise. In chemical and biochemical sensing this problem is exacerbated by the wide range of chemicals to be measured, environments in which to measure them and optical phenomena to be used, and the frequent requirement to make the devices disposable. However, integrated optical approaches have several advantages over optical fibre for chemical sensing, as it is simple to integrate reference sensors and electrodes for reaction control, to print chemically sensitive layers on a chip surface, and to assemble the chip into a complementary microflow system. An integrated optical waveguide is intrinsically sensitive to surface reactions before addition of a cladding, while conventional optical fibre is produced in a way which renders it extremely insensitive to its surroundings.

The approach that we have adopted in exploring the potential for integrated optics in chemical and biochemical sensing has been to study devices which are compatible with planar microflow systems and ultimately can be integrated into the "lab-on-a-chip", which may be connected to instrumentation using optical fibre for a stable optical path and easy "plug & play" operation by those not specialised in waveguide optics, and which lend themselves to use for a wide range of applications by providing a platform for many different chemistries. The permanent connection of optical fibres is relatively costly when compared with "free-space" coupling of light into thin-film waveguides with gratings [2], but brings the advantages of mechanical stability and ease of control of the spatial distribution of the evanescent intensity over the surface of the chip. This approach is not aimed at cheap "single-shot" disposable devices but at arrays of sensors for multiple analytes where the surface chemistry may be regenerated *in situ* using electrochemical or chemical regeneration, allowing repeated use, or is in dynamic equilibrium with the environment. However, it is expected that many of the scientific results may be exploited for use in lower-cost disposable applications. The simple low-cost base technology of ion-exchange in glass has been adopted as a vehicle to realise transducers based upon absorption [3], refractive index [4,5] and fluorescence [6-8] have been realised and their combination with electrochemical techniques using indium tin oxide (ITO) coated and gold-coated devices [3,9] has been demonstrated.

ECIO'05: 12th EUROPEAN CONFERENCE ON INTEGRATED OPTICS
- ABSTRACT -

In this paper a sensor system based upon fluorescence immunoassay on an integrated optical sensor chip will be described as an example of a simple application of integrated optics in biochemical sensing, developed to the point of a prototype instrument which meets a user requirement for pollution monitoring. In contrast to this, ongoing work on integrating electrochemical control and interrogation of chemical reactions at surfaces in a waveguide-coupled surface plasmon resonance sensor will be described, to illustrate the potential of these techniques for fundamental surface studies and ultimately more advanced integrated sensor devices. It is hoped that this will illustrate both the hurdles still to be overcome and the huge potential for applying integrated optical techniques to chemical sensing in the environment, security, medicine and process control.

FLUORESCENCE MULTISENSOR FOR WATER POLLUTION

Fluorescence-based array biosensors hold particular promise where a tagging scheme may be employed, due to their high specificity and tolerance to temperature changes and to non-specific binding. In this work a fibre-pigtailed chip consisting of a channel waveguide circuit which distributes evanescent excitation light to 32 separate sensing patches on the chip surface is used for the single analyte estrone [6], and then for six pollutants simultaneously [7,8]. Estrone pollution, which arrives in waterways as a byproduct of pharmaceuticals, is potentially deleterious to human wellbeing due to its hormonal activity. A characteristic immunoassay calibration curve has been generated that yields a detection limit of 1 ng/L with a range (without dilution) up to about 1 μg/L, and water samples can be analysed directly without time-consuming concentration techniques. A microfluidic system is used to automatically handle the sample injection over the sensor surface, enabling rapid, simultaneous and high-sensitivity fluorescence detection of up to 32 pollutants. A fibre-coupled detection array monitors the 32 separate fluorescence signals, and software controls the laser, fluidics, data acquisition and processing of the fluorescence signals and records the laser power and ambient and chip temperature.

The multisensor chip was fabricated by potassium ion-exchange in BK7 glass following the schematic layout shown in Fig 1. The guides are monomode up to the end of the Y-junction splitter, with parabolic tapers widening to 30μm introduced into each waveguide branch after the Y-junction splitters to reduce the optical power density at the waveguide surface, and hence the rate of fluorophore photobleaching [10]. The 32 sensor windows were opened in a 1μm thick silica isolation layer sputtered onto the surface.

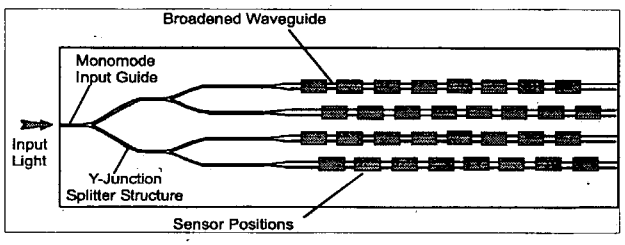

Fig. 1. Schematic diagram of fluorescence sensor chip

The isolation layer prevents excess losses due to contact with the flow cell and environment outside the sensing regions. In order to improve the sensitivity of the sensor, by enhancing the intensity of the excitation light at the waveguide surface in the windows, a 35 nm thick high index film of Ta_2O_5 was deposited over the entire surfaces of the chip by RF sputtering in an Ar/O_2 atmosphere. The ends of the chip were polished to a length of 67mm and a monomode polarisation-maintaining (PM) fibre pigtail with connector was permanently bonded to the input end of the sensor chip.

The system for immunoassay measurements is shown schematically in Fig. 2. Light from a semiconductor laser emitting 5mW at 637±2nm is coupled into the input waveguide of the sensor chip using the fibre pigtail. The evanescent field is able to interact with the analyte in the 32 exposed sensing regions. If a fluorophore is brought within a few 100nm of the sensing spot the evanescent field of the guided light will excite the fluorophore, and a fraction of the resulting fluorescence is collected by an array of 1mm core diameter high numerical aperture polymer optical fibres located directly under the sensor chip. Crosstalk between patches is minimized by ensuring that the emissive regions of adjacent patches are not within the angular acceptance cone (NA) of the fibres. The fluorescence is filtered to remove stray excitation light, detected by a silicon photodiode and low-pass filtered at 1.4Hz. A micro-flow-cell is affixed to the chip over the 32 patches to supply sequences of solutions to the sensor surface. The pumps and valves which supply the solutions, the laser, and the data acquisition system are controlled by a computer integrated with the system. The optical detection limit of the full system, defined as 3×NEP, has been found experimentally to be equivalent to ~500fW of fluorescence power. The fluorophore chosen for this work was Cy5.5 (Amersham Pharmacia). The wavelength shift between the excitation wavelength and the emission wavelength is ~50nm, so that scattered excitation light is straightforward to filter from the signal. Although the wavelength of peak absorption of Cy5.5 is approximately 675nm, it has a flat shoulder in its absorption spectrum near 637nm, reducing the effects of any wavelength variation in the excitation source.

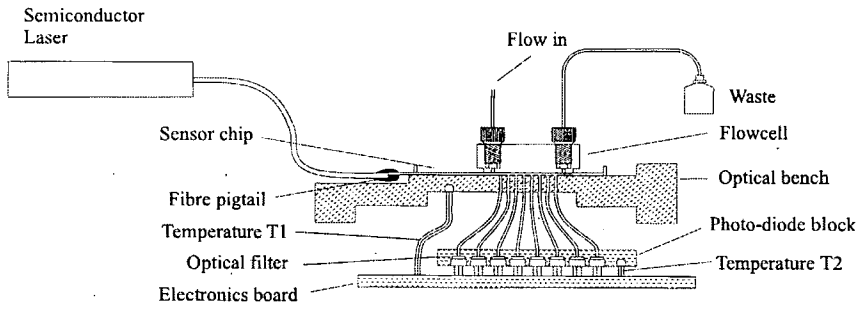

Fig. 2. Experimental apparatus

This multisensor platform may be applied to a wide range of analytes according to the surface attachment protocol. In this case, characterisation of chip and instrument performance for immunofluorescence sensing was carried out with a single analyte, estrone, to assess chip uniformity. The entire sensor surface was chemically modified in order to render the chip specific to estrone. In the case of multiple analytes, each patch will be modified separately by microdispensing specific chemicals only onto the patches, reducing the usage of reagents. An aminodextran layer was coupled to the silanised surface to allow attachment of the specific chemistries. The sensor surface was then immersed in a solution of the analyte derivative, estrone carbonate acid. This procedure leads to a high surface density of binding sites specific to estrone antibodies. Non-specific binding of molecules other than estrone antibodies is limited due to the shielding of the glass surface by the aminodextran.

The performance of the biosensor was demonstrated by measuring the response to eight known concentrations of the analyte estrone in water, ranging from 0 ng/L (blank) to 10 µg/L. 100 µL of antibody solution containing 60 ng/mL of labelled affinity purified polyclonal anti-estrone antibody in 10-fold phosphate buffered saline (PBS) were added to 900 µL of each standard solution and mixed thoroughly to allow the analyte to bind to the fluorescent-labelled antibody molecules, according to its concentration. The incubated solution was then pumped over the sensor surface as described below. Those antibodies which have not been bound to analyte molecules are free to bind to the sensor surface. The output of one sensing channel during a sensor test cycle is shown in Fig. 3, and progressed as follows: A constant flow of PBS was established through the micro-flow-cell, and the background signal, due to laser breakthrough and background fluorescence, was measured. While the incubated sample was being loaded and injected into the flow-cell, the laser was turned off to prevent the onset of photobleaching. After binding of the incubated sample at the sensor surface for ~10 minutes, the cell was flushed with PBS again and the laser turned on, allowing fluorescence from the Cy5.5 dye to be detected.

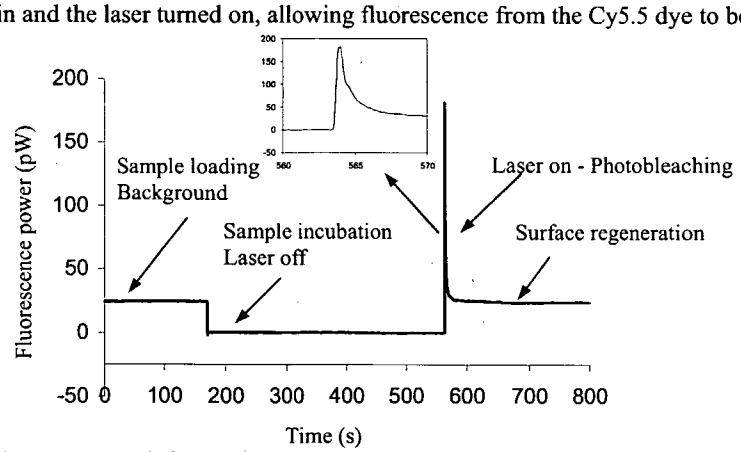

Fig. 3. Sensor test cycle for zero estrone in water (blank) using 6ng/mL anti-estrone

Fig. 3 shows that, once the background has been subtracted, a peak signal of ~155pW was obtained and that this was bleached in a few seconds. Nonetheless, there is no difficulty in acquiring this signal, and the signal to noise ratio is of order 1000. After measurement, the surface was regenerated by 0.5% sodium dodecyl sulphate, adjusted with HCl to pH 1.8, to remove the antibodies bound to the surface, so that another measurement could be carried out, with the entire cycle time taking less than 18 minutes. Surface regeneration may be carried out up to 400 times without significant degradation of the surface chemistry.

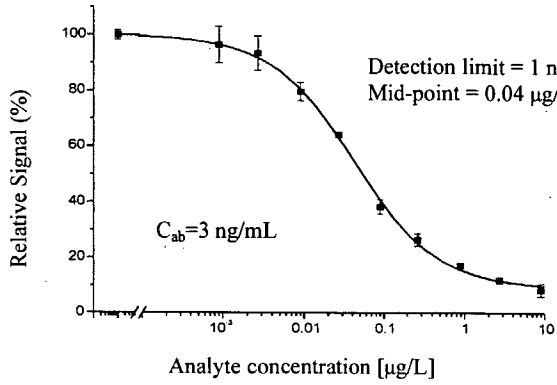

Fig. 4. Averaged calibration curve for estrone, using 3ng/mL anti-estrone

A calibration curve for normalised fluorescence power against estrone concentration was obtained by repeating this procedure using the 3ng/mL dye-labelled antibodies and water samples containing estrone, prepared as described above. The averaged data were fitted to a logistic function, representing a close approximation to the shape of a typical immunoassay curve, and an example is given in Fig. 4, which shows the estrone calibration curve for one sensing patch normalised to the mean of the signals for the blanks. The detection limit (LoD) for estrone for this sensing patch, taken to be the concentration at which the signal has fallen below the blank value by thrice the standard deviation of the blanks was found to be just below 1 ng/L. Concentrations up to 1µg/L are measurable and higher concentrations could be measured by dilution.

The first multi-analyte test of this sensor, successfully carried out with a mixture of six analytes, atrazine, bisphenol A, estrone, isoproturon, sulphamethizole, and propanil [7,8], limited by the availability of antibodies is shown in Figure 5. In this case the specific chemistries were microdispensed onto the sensing windows. The highest detection limit was 20ng/L, which is within the requirements of EU legislation for organic pollutants, and it is expected that improvements in sample handling and signal processing will reduce this further. The ability to regenerate the sensor automatically after an assay, as part of an automated protocol, means that the sensor and system may be left unattended for months, in normal operation, before a chip needs replacing. There is potential for further miniaturisation, increased integration and reduced use of reagents as the fluorescent signal is obtained from an irradiated area of ~0.05mm^2 and volume below 20pL.

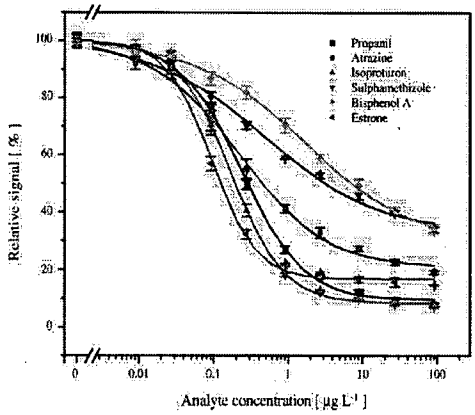

Fig. 5. Fluorescent signal vs. concentration for 6 pollutants

Monitoring water quality and identifying pollution sources are emerging as important tasks in the future management of rivers, which are major sources of water for human consumption. This approach may also be applied to a wide range of biochemical analyses in other applications where the use of fluorescent-labelled reagents is possible. The automated regeneration of the sensor surface for repeated use avoids immediate disposal of the sensor chip and may render the cost per measurement competitive with laboratory-based techniques. Further work on more efficient collection of the emitted fluorescence is planned, and the other key directions are now in improving control of the fluidics, use of improved fluorophores or quantum dots, and more compact instrumentation for non-remote medical applications.

ECIO'05: 12th EUROPEAN CONFERENCE ON INTEGRATED OPTICS
- ABSTRACT -

ELECTROCHEMICALLY CONTROLLED WAVEGUIDE SURFACE PLASMON RESONANCE

Direct, unlabelled, measurements of biochemical binding at surfaces are most often made by detecting changes in the thickness or refractive index of an adlayer. The highly successful optical biosensor instrument (Biacore) employs surface plasmon resonance (SPR) to detect these changes [11], and a variety of sensors based upon waveguide interferometry have been demonstrated and commercialised [12,13]. There is a wealth of experience in the user community of modifying gold surfaces for biochemical analyses and in using SPR and electrochemical techniques for biosensing and fundamental studies of biomolecular interactions. There is also a potential advantage in combining two physical sensing principles in one measurement to confirm the result and help to reduce "false positives" [14]. In this work we have sought (i) to integrate SPR into a waveguide format, following the original approach of Kreuwel [15], to provide a rugged, miniature, "sensorised" version of a conventional SPR instrument and (ii) to study the simultaneous electrochemical control and measurement of surface reactions, using the gold film which supports the surface plasma wave as a working electrode [3,9].

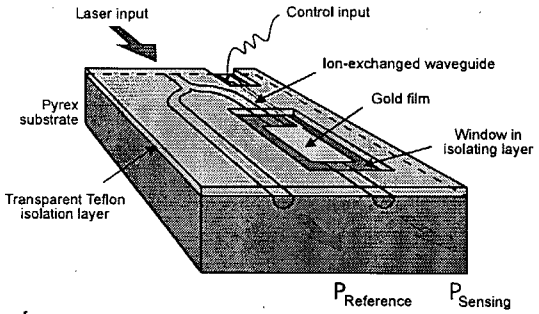

Fig. 6. Schematic diagram of waveguide SPR sensor

A schematic diagram of the basic waveguide SPR device is shown in Figure 6. Monomode potassium ion-exchanged waveguides similar to those above have been used again for simplicity. The waveguide is split to provide a reference output to allow compensation for input power fluctuations. The signal branch is coated with a 35nm-65nm thick gold electrode of length between 1 and 3 mm, to which an electrical connection is provided. The chip is coated with ~1μm of Teflon AF (n≈1.33) (which is easily removed) to isolate the waveguides and electrode from the analyte and the flow-cell to be clamped on the chip.

Refractive index changes at the gold surface alter the velocity of the surface plasma wave on that surface, changing the degree of phase-matching between the waveguide mode and the SPW, and this is observed as a strong resonant absorption vs. refractive index [16], similar to that in the conventional Kretschmann configuration for fixed incident angle. Choice of the low index Pyrex substrate (n≈1.47) and operation at a wavelength of 630-640nm results in the device being close to phase-matched in an aqueous medium (n≈1.33). Steps may be taken to phase-match at other wavelengths and in other media, but this configuration is the simplest. This device has been used to detect organic pollutants in water in a similar way to the fluorescence sensor above, without using a fluorescent tag, and detection limits of ~100ng/L were obtained [5].

Initial combined optical/electrochemical measurements using this device were designed to establish the potential of the technique, employing well-known chemistry. Underpotential electrochemical deposition (UPD) of monolayers of metal adsorbates on noble metal surfaces occurs below the Nernst potential required for electroplating, when the adsorbate atoms are bonded to the noble metal atoms more strongly than to a surface of the adsorbate metal [17]. The electroadsorption process may be expressed as: $Cu^0(ads) \leftrightarrow Cu^{2+}(sol) + 2e^-$, where ads and sol refer to adsorbed copper and copper ions in solution. An open cylindrical silica cell was clamped to the waveguide surface and filled with 10^{-3} M Cu^{2+} in 0.1 M perchloric acid (n = 1.334). A three-electrode cyclic voltammetry circuit was established by introducing a platinum wire counter electrode and a saturated calomel (SCE) reference electrode into the cell, with the gold film pads acting as the working electrodes. Permanent contact was made to the gold electrodes outside the cell at the edge of the substrate. All three electrodes were connected to a conventional potentiostat, allowing the potential of the working electrode with respect to the reference electrode, E, to be controlled and the current, I, through the working electrode to be measured. Light at 633 nm was coupled into the device in the TM polarisation using a polarisation-maintaining fiber.

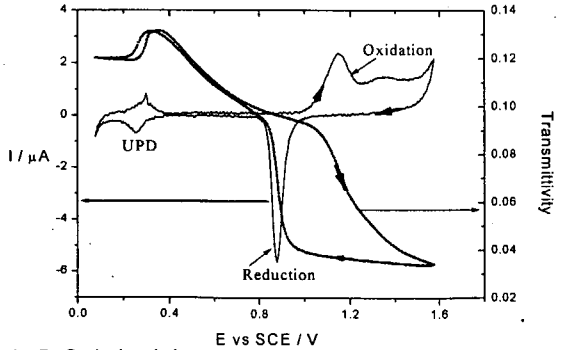

Fig. 7. Optical and electrochemical response of waveguide SPR sensor

Figure 7 shows the optical transmission and the current against the applied potential after several voltage cycles. The first part of the potential scan, from 0.5 V to 1.6 V, causes the anodic oxidation of the gold surface, as is shown by the current peak at about 1.1 V and the corresponding drop in transmission. The cathodic scan shows the corresponding reduction peak in the current and increase in the optical transmission. The reduction is completed at about 0.7 V where the optical transmittance has returned to its pre-oxidation value. As the potential decreases from 0.7 V to 0.4 V, the transmittance increases due to the alteration of the ionic distribution of the double layer at the metal – electrolyte interface. This ionic redistribution involves the chemisorption of anions at the gold, and results in a small displacement current. At a potential of 0.24 V a peak in the current is observed, which is due to the deposition of a monolayer of Cu onto the gold film surface. The deposition of this monolayer of approximately 0.3 nm thickness gives rise to a 10% drop in the optical transmittance. Integration of the peak current over time during deposition gives a charge of 0.41 mC / cm^2, which is close the theoretical value of 0.44 mC / cm^2 for a monolayer of Cu^{2+} ions transferring two electrons per ion to an ideal Au (111) surface. The direction of the potential scan is reversed at 0.1 V and a peak in current is observed at 0.29 V, corresponding to stripping of the Cu monolayer, and the transmittance increases correspondingly.

The processes involved in the electrochemical oxidation and reduction of a gold surface and the underpotential deposition of Cu^{2+} on gold may be continuously monitored in-situ using with high sensitivity, with complementary information being provided by the electrochemical and optical techniques, and the results compare favorably with those obtained using ellipsometry and reflectance measurements [18-20]. We believe that this device has great potential as a platform upon which to construct a variety of biological sensors. As a further step towards the realisation of such biosensors, we have studied the self-assembly of monolayers of an alkanethiol and their electrochemical desorption. Enzymes and lipid membranes, for example, may be attached to the gold electrode using alkanethiols while keeping them directly 'wired' to the electrode enabling electrochemical reactions to be carried out. The electrochemical desorption of the alkanethiol may provide a route to patterning biological sensing materials to be attached to the sensor surface.

A cell containing 10 mM sulphuric acid, an Hg/Hg_2SO_4 reference electrode and a gold wire counter electrode was clamped to the chip. The working electrode was ramped from 0 V up to 1.1 V and back down to 0 V repeatedly using a scan rate of 20 mV/s and the signal (P_{sig}) and reference (P_{ref}) powers giving the transmission (P_{sig}/P_{ref}), and potential and current were recorded on a PC. Ten cycles were performed in order to clean the gold of any surface impurities before deposition of the decanethiol. The decanethiol monolayer was formed by self-assembly from a 1mM solution of decanethiol in ethanol over 12 h. Figure 8 shows both the electrochemical (solid line) and the optical (dotted line) response to cyclic voltammetry in acid for a gold electrode coated with a decanethiol monolayer over ten cycles. The first electrochemical cycle shows a small oxidation current and a correspondingly small reduction current with a peak of –17 nA at 0.4 V.

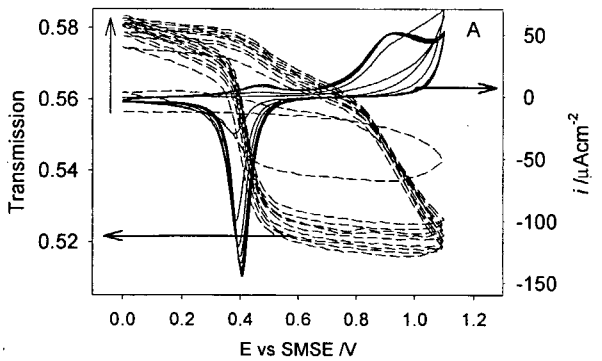

Fig. 8. Sequential voltammograms and optical signal showing progressive desorption of alkanethiol

For subsequent cycles, larger oxidation and reduction currents are observed, until reproducible cyclic voltammograms are obtained with peak currents of 85 nA, similar to those for an untreated gold film. The first optical cycle also shows only a small modulation in transmission compared to the data for an untreated gold surface, and the transmission at the end of each cycle (0V) increases for each subsequent cycle. After ten cycles the shape and magnitude of both the optical and electrochemical data are similar to that measured for the untreated film. Initially a small oxidation and reduction current are measured, because the thiol layer blocks the flow of charge to the gold working electrode. However as coverage of the thiol is not perfect, some of the gold surface is available to take part in the oxidation/reduction reaction. At ~1.0V some desorption of the thiol film takes place. After ten cycles the thiol is completely stripped off and the CV is almost identical to that of the untreated gold film. These results have two principal implications for chemical sensing, the first that the

attachment and detachment of a monomolecular film may readily be detected by waveguide surface plasmon resonance, and the second that in a single chip multisensor array, electrochemical desorption may potentially be used to commit each sensing patch to a different surface chemistry. Our aim is to develop this device into a biosensor for detection of the enzyme phospholipase A_2, which is implicated in inflammatory diseases such as asthma and cystic fibrosis, using a lipid membrane attached to the sensor surface with the alkanethiol.

CONCLUSION

Chemical and biochemical sensing is exploiting advances in integrated optical technologies to realise compact robust multisensor devices with high sensitivity. Integrated optical chemical sensors are beginning to become commercially available and there is a huge variety of applications for such sensors, with potentially large markets for solutions which compete with existing approaches. In this paper two approaches to chemical and biochemical sensing have been outlined, one a simple high-sensitivity platform for a multitude of fluorescence-based chemical sensing schemes, and the other a more advanced approach which combines monitoring of electrochemical and optical parameters, building upon the well-established and accepted technique of SPR biosensing.

ACKNOWLEDGEMENTS

Support by the European Union 5th Framework Programme, Energy, Environment & Sustainable Development, and the UK Engineering and Physical Sciences Research Council (EPSRC), and the contributions of many colleagues are gratefully acknowledged.

REFERENCES

1) B. Culshaw, 'Optical fiber sensor technologies: opportunities and - perhaps - pitfalls', Journal of Lightwave Technology, **22**, 39-50 (2004).
2) G.L. Duveneck, A.P.Abel, M.A. Bopp, G.M. Kresbach and M. Ehrat, "Planar waveguides for ultra-high sensitivity of the analysis of nucleic acids," Anal. Chim. Acta **469**, 49-61 (2002).
3) C.Piraud, E.K.Mwarania, G.Wylangowski, K.O'Dwyer, D.J.Schiffrin, & J.S.Wilkinson, "Optoelectrochemical Thin-Film Chlorine Sensor Employing Evanescent Fields on Planar Optical Waveguides", Analytical Chemistry, **64**, 651-655, (1992).
4) B.J.Luff, J.S.Wilkinson, J.Piehler, U.Hollenbach, J.Ingenhof & N.Fabricius, "Integrated Optical Mach-Zehnder Biosensor", Journal of Lightwave Technology, **16**, 583-592 (1998).
5) R.D.Harris, B.J.Luff, J.S.Wilkinson, J.Piehler, A.Brecht, G.Gauglitz & R.A.Abuknesha, "Integrated Optical Surface Plasmon Resonance Immunoprobe for Simazine Detection", Biosensors & Bioelectronics, **14**, 377-386 (1999).
6) P. Hua, J.P. Hole, J.S. Wilkinson, G. Proll, J. Tschmelak, G. Gauglitz, M.A. Jackson, R. Nudd, H.M.T. Griffith, R.. Abuknesha, J.Kaiser and P. Kraemmer, "Integrated optical fluorescence multisensor for water pollution", Optics Express, **13**, 1124-1130 (2005).
7) J Tschemelak, G Proll, J Riedt, J Kaiser, P Kraemmer, L Barzaga, JS Wilkinson, P Hua, JP Hole, R Nudd, M Jackson, R Abuknesha, D Barcelo, S Rodriguez-Mozaz, M Lopez de Alda, F Sacher, J Stien, J Slobodnik, P Oswald, H Kozmenko, E Korenkova, L Tothova, Z Krascsenits & G Gauglitz, "Automated Water Analyser Computer Supported System (AWACSS) Part I: Project objectives, basic technology, immunoassay development, software design and networking", Biosensors & Bioelectronics, **20**, 1499-1508 (2005).
8) J Tschemelak, G Proll, J Riedt, J Kaiser, P Kraemmer, L Barzaga, JS Wilkinson, P Hua, JP Hole, R Nudd, M Jackson, R Abuknesha, D Barcelo, S Rodriguez-Mozaz, M Lopez de Alda, F Sacher, J Stien, J Slobodnik, P Oswald, H Kozmenko, E Korenkova, L Tothova, Z Krascsenits & G Gauglitz, "Automated Water Analyser Computer Supported System (AWACSS) Part II:Intelligent, remote-controlled, cost-effective, on-line, water monitoring measurement system", Biosensors & Bioelectronics, **20**, 1509-1519 (2005).
9) J.C.Abanulo, R.D.Harris, A.K.Sheridan, P.N.Bartlett & J.S.Wilkinson, "Waveguide surface plasmon resonance studies of surface reactions on gold electrodes", Faraday Discuss., **121**, 139–152 (2002).
10) R.D. Harris , G.R.Quigley, J.S. Wilkinson, A. Klotz, C. Barzen, A. Brecht, G. Gauglitz, R. A. Abuknesha, "Waveguide immunofluorescence sensor for water pollution analysis," Chemical Microsensors and Applications, **3539**, 27-35 (1989).
11) M. Malmqvist, "Biospecific interaction analysis using biosensor technology", Nature, **361**, 186-187 (1993).
12) M.J. Swann, L.L. Peel, S. Carrington, et al. "Dual-polarization interferometry: an analytical technique to measure changes in protein structure in real time, to determine the stoichiometry of binding events, and to differentiate between specific and nonspecific interactions", Anal. Biochem., **329**, 190-198 (2004).
13) R.J. Leatherbarrow & P.R. Edwards, "Analysis of molecular recognition using optical biosensors", Curr. Opin. Chem. Biol., **3**, 544-547 (1999).
14) G.M. Murray & G.E. Southard, "Sensors for chemical weapons detection", IEEE Instrumentation and Measurement Magazine, **5**, 12-21, (2002).

15) H.J.M. Kreuwel, P.V. Lambeck, J.M.M. Beltman & Th. J.A. Popma, "Mode coupling in multilayered structures applied to a chemical sensor and a wavelength-selective directional coupler", Proc 4th Int. Conf. Integrated Optics, Glasgow, 217-220 (1987)
16) J.Ctyroký, J.Homola, P.V.Lambeck, S.Musa, H.J.W.M.Hoekstra, R.D.Harris, J.S.Wilkinson, B.Usievich & N.M.Lyndin, "Theory and Modelling of Optical Waveguide Sensors Utilising Surface Plasmon Resonance", Sensors & Actuators B, **54**, 66-73 (1999).
17) J.G. Xu and X.W. Wang, "Study of copper underpotential deposition on Au(111) surfaces", Surf. Sci., **408**, 317-325 (1998).
18) Y.Iwasaki, T. Horiuchi, M.Morita & O. Niwa, "Time differential surface plasmon resonance measurements applied for electrochemical analysis", Electroanal., **9**, 1239-1241 (1997).
19) W. Visscher and A.P. Cox, "Ellipsometry of metal deposition", Electrochim. Act., **37**, 2245-224 (1992).
20) K. Takamura, F. Watanabe and T. Takamura, "An interpretation on the origin of the specular reflectance change caused by the submonolayer formation of foreign metals on some precious metal electrodes", Electrochim. Act., **26**, 979–987 (1981).